Talanta 105 (2013) 409–416

Contents lists available at SciVerse ScienceDirect

Talanta

journal homepage: www.elsevier.com/locate/talanta

Imprinted polymers with cyclodextrin pseudo-polyrotaxanes as pseudo-supports for protein recognition

Minjie Guo [a,*], Xin Hu [a], Zhi Fan [a], Jing Liu [a], Xiaocong Wang [a], Ying Wang [b], Huaifeng Mi [b]

[a] Department of Chemistry, College of Sciences, Tianjin University of Science and Technology, Tianjin 300457, PR China
[b] Key Laboratory of Functional Polymer Materials, Ministry of Education of China, Institute of Polymer Chemistry, Chemical School, Nankai University, Tianjin 300071, PR China

ARTICLE INFO

Article history:
Received 8 August 2012
Received in revised form
10 October 2012
Accepted 20 October 2012
Available online 1 November 2012

Keywords:
Assistant recognition polymer chains
Cyclodextrins pseudo-polyrotaxane
Molecularly imprinted polymer
Poly (vinyl alcohol)
Protein adsorption

ABSTRACT

We report a novel approach for preparing protein molecularly imprinted polymers (MIPs) with cyclodextrin pseudo-polyrotaxanes (CD-PPRs) as pseudo-supports, which are formed by self-assembling assistant recognition polymer chains with γ-cyclodextrins. The conformation of the CD-PPRs was characterised by 2D-NOESY, TGA and WAXD. To prepare MIPs, template bovine serum albumin (BSA) was first selectively assembled with modified CD-PPRs to form complexes in the presence of Cu ions. These assemblies were then immobilised by the polymerisation of acrylamide as the monomer and *N,N′*-methylenebisacrylamide as the cross-linker to prepare protein MIPs. The amount of BSA template adsorbed initially increased with the increase in the amount of CD-PPR and then decreased with the further increase in the CD-PPR content. To obtain the specific adsorption protein, MIPs were washed with KCl solutions of different concentrations. The results of sodium dodecyl sulphate–polyacrylamide gel electrophoresis showed that the specific adsorption proteins could be collected with a 0.500 mol L^{-1} KCl solution. The recognition specificity to the template relies on the spatial configuration constructed by CD-PPR and metal ions. Finally, this imprinted polymer was used to purify the template from the protein mixtures containing either two (BSA and ovalbumin) or four (BSA, ovalbumin, soybean trypsine inhibitor and lysozyme) different proteins. Both experiments have demonstrated MIPs high selectivity.

1. Introduction

The purification of modern biotechnology products has continuously garnered much attention due to its high cost, which is almost 70–90% of the total product cost. Molecular imprinting, an economical, simple and stable technology, has become a powerful method for the separation of proteins [1–3]. Protein molecularly imprinted polymers (MIPs) possess specific recognition sites to the target protein in polymer networks by the polymerisation of a cross-linker and functional monomers [4–6]. To date, the most successful protein imprinting methods have been performed by surface imprinting on supports, which are most typically silica particles [7–9] and microspheres [10,11]. The particles diameters of the majority of these supports exceed the millimetre scale, while the diameter of a spherical protein with a polypeptide chain is approximately 10 nm [12]. From the point of view of support dimensions, the method of surface imprinting on the supports is insuitable for protein imprinting. Even if the specific recognition of the target protein is successful in separation, the relatively large supports require excessive eluent during the enrichment of the target protein. In recent years, some new studies for MIPs have been developed and been reviewed [13]. Atomic force microscopy spectroscopy has been used to measure the specific binding forces between template protein and receptor sites created at the surface of polymer films by molecular imprinting [14]. Micron scale microspheres have been prepared for lysozyme imprinting [15]. The MIPs coated CdTe quantum dots integrate the advantages of the high selectivity of the molecular imprinting and strong fluorescence property of the quantum dots [16].

Herein, we report a novel approach for preparing protein MIPs with cyclodextrin pseudo-polyrotaxanes (CD-PPR) as pseudo-supports, which were formed by self-assembling assistant recognition polymer chains (ARPCs) with γ-cyclodextrins (γ-CDs). In addition, metal ions were introduced and helped to form more stable complexes with the template molecules via multiple-site coordination interactions.

Cyclodextrins (CDs, the cyclic oligomers of glucose units, including α-CD, β-CD and γ-CD, according to the number of glucose units) chemistry has garnered increasing attention over the past twenty years, and CD is one of the most widely used supramolecular chemistry hosts. Supramolecular chemistry has recently expanded to supramolecular polymer chemistry [17]. The phenomenon of polymer inclusion complexes is now well known [18,19]. Polyrotaxanes, chemical species featuring an intriguing supramolecular architecture, are usually obtained from CDs threaded around a polymer chain that by blocking penetrates their empty cavities; alternatively, pseudo-polyrotaxanes can be

* Corresponding author. Fax: +86 22 60601179.
E-mail address: guomj@tust.edu.cn (M. Guo).

0039-9140/$ - see front matter © 2012 Elsevier B.V. All rights reserved.
http://dx.doi.org/10.1016/j.talanta.2012.10.061

obtained without blocking. It has been demonstrated that CD molecules are regularly aligned and cooperatively bind the target during molecular imprinting towards amino acid derivatives and protein [20,21]. In this work, γ-CD was chosen as a cyclic component because of its larger internal diameter relative to that of α-CD, β-CD for the construction of CD-PPRs, with the aim of preparing protein imprinted polymers.

Polyvinyl alcohol (PVA) has been observed to form inclusion complexes with γ-CD [22]. Low-molecular-weight (LMW) PVA has been employed as a linear polymer guest to construct CD-PPRs in this work. PVA was selected as an ARPC because it is a water-soluble and biocompatible polymer that has found numerous applications in the biochemical and biomedical fields [23]. Furthermore, the chain length of PVA can be easily controlled via the polymerisation of vinyl acetate. As is known, the molecular weight of PVA is based on the length of the initial vinyl acetate polymer and the degree of alcoholysis. In our previous work, a PVA graft copolymer was introduced as an ARPC to enhance the recognition specificity in the protein imprinting process [24–26].

Fig. 1 shows the procedure followed to synthesise the protein imprinted polymers. First, the ARPCs were assembled with γ-CD to form CD-PPRs, in which LMW PVA acted as an ARPC and was synthesised easily by traditional free radical polymerisation. Second, the template protein was assembled with the modified CD-PPRs (functionalised with acryloyl chloride) selectively to form protein complexes in the presence of Cu ions. Third, protein MIPs were prepared with acrylamide as the monomer in the presence of protein complexes.

2. Experimental methods

2.1. Materials

Vinyl acetate (VAc), 2,2′-Azobisisobutyronitrile (AIBN), methanol (MeOH), ethanol, and *N*,*N*′-dimethylsulphoxide (DMSO) were purchased from KRS Chemical Reagent Ltd. (Tianjin, PR China), and all were of analytical grade. *N*,*N*′-methylene bisacrylamide (MBA), acrylamide (AM), acryloyl chloride, and sodium dodecyl sulphate (SDS) were produced from Sigma-Aldrich Corporation. γ-CD was purchased from Cerestar Co. Proteins were produced by Worthington Biochemical Corporation (USA). Bovine serum albumin (BSA), ovalbumin (OVA), soybean trypsine inhibitor (SBTI), lysozyme (LYS) and protein marker (mid range) were purchased from Shanghai Sangong Biotechnology Ltd. All other chemicals and solvents were obtained from commercial sources and were used as received.

2.2. Synthesis of LMW PVA

LMW PVA was synthesised with VAc as the monomer via free radical polymerisation as described in reference [24]. At a ratio of $V_{MeOH}/V_{VAc}=4.60$ and an initiator AIBN concentration of 8.50 mmol L^{-1}, the resultant product was obtained, and the degree of alcoholysis was approximately 85%. The molecular weight of the synthesised PVA, the linear polymer guest, was determined using a Waters 410 GPC system. As shown in Fig. 2, $M_p=8772$ and $M_w/M_n=1.40$.

2.3. Preparation of CD-PPR

To a saturated aqueous solution of γ-CD (20.0 mL) stirred at 80 °C, 1.00 g PVA was added. The mixtures were kept at 80 °C for 12 h and at 25 °C for 12 h under moderate stirring. This process was repeated five times. After 120 h, water was partially removed from the reaction system with a rotary evaporator to yield a concentrated solution. The clear solutions were poured into alcohol for precipitation and then separated by centrifugation with a 20PR-52D high-speed centrifuge made by Japan Hitachi Company. Then, the products were dissolved in water at room temperature and thereafter separated by centrifugation. The product was dried to constant mass in an oven at 60 °C, and CD-PPR was obtained. A volume of 1.0 mL acryloyl chloride was added to a 10% (*w*/*v*) DMSO solution of CD-PPR (10.0 mL), and the reaction was carried on for 4 h at 40 °C under stirring. After being

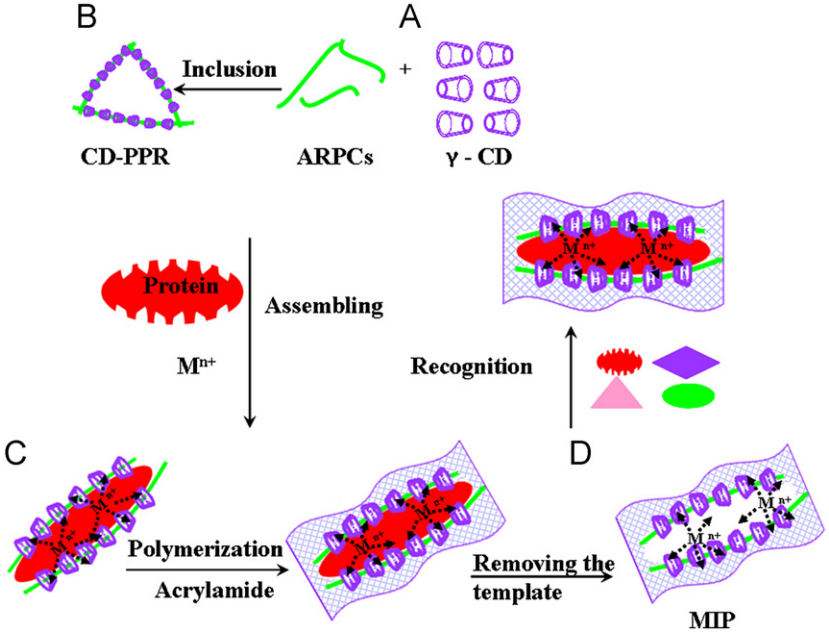

Fig. 1. Protocol for protein imprinting with cyclodextrin pseudo-polyrotaxanes as pseudo-supports. (A) Cyclodextrin pseudo-polyrotaxane (CD-PPR) formation was designed to occur between PVA and γ-CD. PVA, whose degree of polymerisation was approximately 200 and degree of alcoholysis was approximately 85%, was used as an ARPC in this work (see the Supporting Information). (B) The assembly of the CD-PPR skeleton and the template protein in the presence of metal ions. (C) Illustration of outlining MIPs matrix. (D) MIPs for target protein recognition.

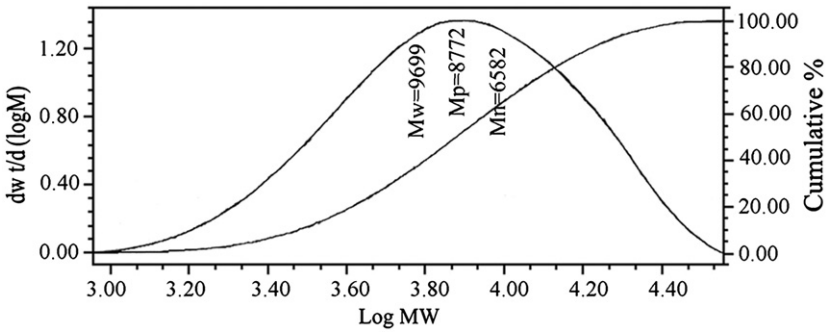

Fig. 2. GPC analysis of the synthesised PVA.

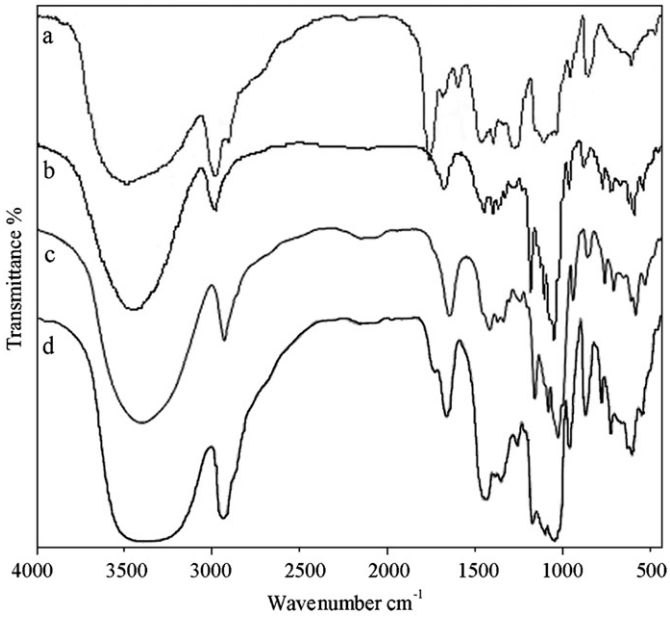

Fig. 3. FTIR spectra of (a) PVA, (b) pure γ-CD, (c) CD-PPR and (d) acrylated CD-PPR.

precipitated and washed, the modified CD-PPR was dried in a vacuum at room temperature to a constant mass.

2.4. Characterisation of CD-PPR

To confirm the structure of CD-PPR, the assembly behaviour of this complex was comprehensively investigated by 2D-NOESY, thermogravimetric analysis (TGA), and wide-angle X-ray diffraction (WAXD). 2D-NOESY spectra were recorded on a Unity-plus-400 (400 MHz) spectrometer. Thermal analyses were performed with a Perkin-Elmer Pyris 1 thermogravimetric analyser. The thermal decomposition of the samples was recorded between 25 to 500 °C at a heating rate of 20 °C min^{-1}. Nitrogen was used as the purge gas. WAXD patterns were obtained under ambient conditions on a Rigaku D/max+Adiffractometer with a nickel-filtered Cu *Kα* radiation source (λ=1.54 Å). The supplied voltage and current were set to 30 kV and 20 mA, respectively. A Nicolet 510P FTIR spectrometer was utilised to obtain the infrared spectra of samples mixed into potassium bromide and pressed into pellets. The spectra were recorded over the range of 4000–400 cm^{-1}, with a resolution of 2 cm^{-1} using 64 scans (Fig. 3).

2.5. Preparation of the protein imprinted polymers

In the first step, modified CD-PPR was added to 10.0 mL buffer (0.010 mol L^{-1} NaH_2PO_4/Na_2HPO_4, pH 6.5) and then treated with a copper sulphate solution (0.500 mol L^{-1}) at room temperature (Table 1). The solution was magnetically stirred, and BSA (template molecule, 80 mg) was then dissolved; the mixture was rotated at 4 °C for 1 h for the preorganisation of the protein and CD-PPR-Cu^{2+} complex.

Table 1
Functional monomer composition and synthesis parameters for BSA MIPs.

Numbers	AM (g)	MBA (g)	BSA (g)	APS (g)	CD-PPR (g)	Cu^{2+}(μL)[a]
cp-MIP1	1.00	0.50	0.08	0.075	0.30	10.0
cp-MIP2	1.00	0.50	0.08	0.075	0.60	10.0
cp-MIP3	1.00	0.50	0.08	0.075	0.90	10.0
cp-MIP4	1.00	0.50	0.08	0.075	1.20	10.0
cp-MIP5	1.00	0.50	0.08	0.075	1.00	20.0
cp-MIP6	1.00	0.50	0.08	0.075	1.00	30.0
cp-MIP7	1.00	0.50	0.08	0.075	1.00	40.0
NIP	1.00	0.50	0	0.075	0	0
a-MIP	1.00	0.50	0.08	0.075	0	0
CD-MIP	1.00	0.50	0.08	0.075	1.00	0

[a] Concentration of Cu^{2+} = 0.500 mg mL^{-1}; Volume of phosphate buffer = 10 mL;

To the above-mentioned buffer were added 1.00 g of AM and 0.50 g of MBA, and the mixture was stirred for 1 h with N_2 ventilation to remove O_2. After adding ammonium persulphate, the solution was cooled in an ice bath for 2–3 min. Then, a Na_2SO_3 solution was added, and the reaction was allowed to proceed at 4 °C for 3 h under stirring and N_2 protection. To remove the unreacted monomers and other ingredients, the resultant MIPs were washed with phosphate buffer. After cleaning MIPs, the template was removed from the MIP matrix using a 2.0 mol L^{-1} KCl solution (pH 8.0) until no BSA adsorption was measured in the washing solution at 278 nm using a UV/Vis spectrophotometer produced by the Beijing Liuyi instrument factory. Protein MIPs with CD-PPRs as ARPCs (*cp*-MIP) were obtained.

For the controls, MIPs without ARPCs (*a*-MIP) and MIPs with only acrylated cyclodextrin (CD-MIP) were prepared and treated in exactly the same way. Non-imprinted (NIP) polymer was also prepared in the absence of BSA using the same polymerisation procedure discussed above.

2.6. Characterisation of MIPs

The morphologies of the dried polymers were investigated by scanning electron microscopy (SEM). The polymers were coated with gold and examined using an *S*-3500N SEM produced by Hitachi Company.

2.7. BSA adsorption experiments and template rebinding

The wet cp-MIP (1.00 g) was first incubated in phosphate buffer solution at pH 6.5. Then, 10.0 mL of a 0.500 mg mL^{-1} BSA

protein solution was added and allowed to equilibrate at 4 °C for 15 h under end-over-end rotation. The protein concentrations of the supernatant solutions were measured at 278 nm using the UV/Vis spectrophotometer. The apparent amount of adsorbed protein was calculated from the following formula:

$$Q = \frac{(c_0 - c) \times V}{m}$$

where Q is the apparent amount of protein adsorbed onto a unit mass of wet polymer (mg g^{-1}), c_0 and c are the concentrations of protein in the initial and equilibrium solutions, respectively (mg mL^{-1}), V is the volume of the solutions treated (mL), and m is the mass of wet polymer (g).

To test the reusability of cp-MIP, the BSA adsorption–desorption procedure was repeated 4 times. After one adsorption–desorption cycle, the cp-MIP was washed with a 2.0 mol L^{-1} KCl solution for 60 min. After this procedure, cp-MIP was washed with deionised water for 30 min and then equilibrated with a 0.010 mol L^{-1} phosphate buffer for the next adsorption cycle proceeding still at 4 °C.

2.8. Selectivity experiments and elution procedure experiments

To determine the adsorption specificity, competitive adsorptions of BSA from the protein mixture were also studied in buffer solution. Wet protein imprinted polymer (1.00 g) and 1.0 mL of the protein mixture (containing either two or four different proteins, with a protein concentration of 0.500 mg mL^{-1} each) were incubated at 4 °C for 15 h under end-over-end rotation. The polymers were washed twice with 1.0 mL of a 0.10 mol L^{-1} phosphate buffer, twice with 1.0 mL of a 0.15 mol L^{-1} KCl solution, and then three times with 1.0 mL of a 0.500 mol L^{-1} KCl solution. Ten microlitres of eluent was subjected to sodium dodecyl sulphate–polyacrylamide gel electrophoresis (SDS-PAGE) analysis (gels: 12.0%) using an *E*-865 Electrophoresis System produced by Belgium Consort Company, and the proteins were visualised using Coomassie brilliant blue (CBB). The decolorisation shaker used was made by Nanjing University in China.

3. Results and discussion

3.1. Characterisation of the CD-PPR

3.1.1. 2D-NOESY spectrum

To obtain detailed information about the structure of the CD-PPR, we recorded its 2D-NOESY spectrum. As illustrated in Fig. 4, the NOESY spectrum displayed clear NOE cross-peaks between the *H*-5 and *H*-3 of cyclodextrin and the H belonging to the methylene group of PVA (peaks A). Thus, the results of the NOESY experiment support the formation of a host-guest inclusion complex between PVA and γ-CD.

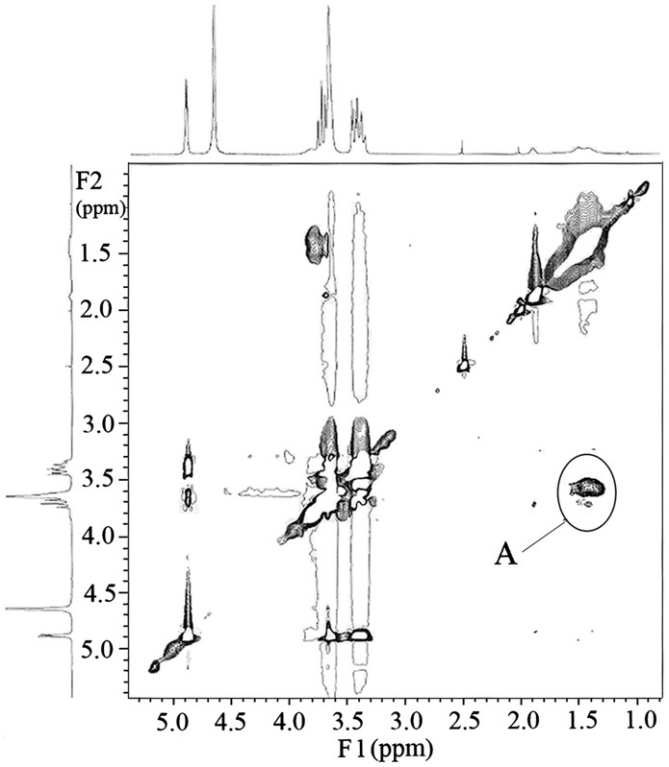

Fig. 4. 2D-NOESY spectrum (400 MHz) of CD-PPR.

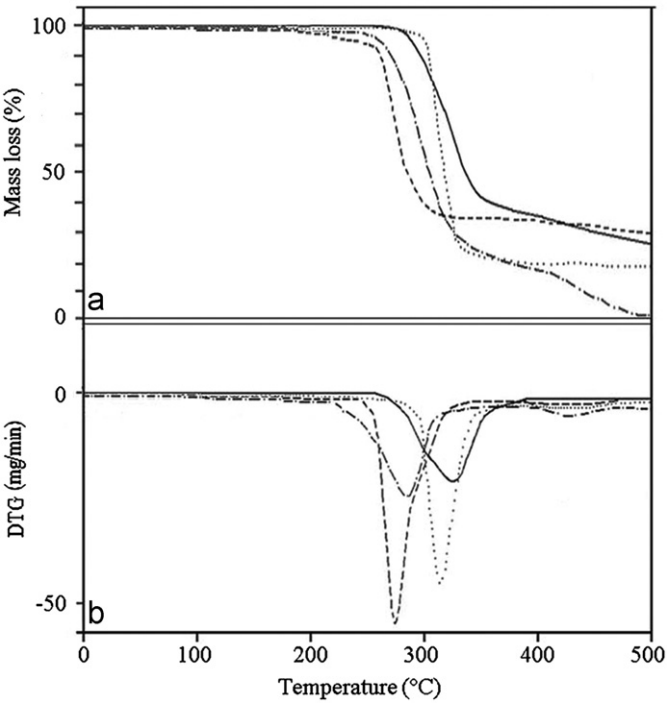

Fig. 5. (a) TGA scans of samples. (b) First derivative of TGA weight loss. (…) pure γ-CD; (—) CD-PPR; (— •) PVA/γ-CD mixture; and (- - -) PVA.

3.1.2. TGA analysis

Fig. 5 shows the TGA scans for γ-CD, CD-PPR, PVA/γ-CD physical mixture and PVA. As shown, the initial decomposition of the CD-PPR started at 289 °C, which was intermediate between the decomposition temperatures of PVA (256 °C) and γ-CD (301 °C). This phenomenon of higher decomposition temperatures for CD-PPR may imply that the polymer chains existed inside the CD-PPR channels, thereby improving the thermal stability of PVA. These results can be attributed to the hydrogen bonds among the CD molecules and ARPCs molecules. Furthermore, it could be observed that the PVA/γ-CD physical mixture started to decompose at 264 °C, which was 25 °C lower than the onset of thermal decomposition in CD-PPR, at approximately 289 °C. Moreover, the curve slope of CD-PPR was smaller than that of CD and that of PVA; the results indicate that the rate of weight loss of CD-PPR was lower.

3.1.3. WAXD analysis

Fig. 6 presents a comparison of the WAXD patterns observed for PVA, the physical mixture of PVA and γ-CD, CD-PPR and pure

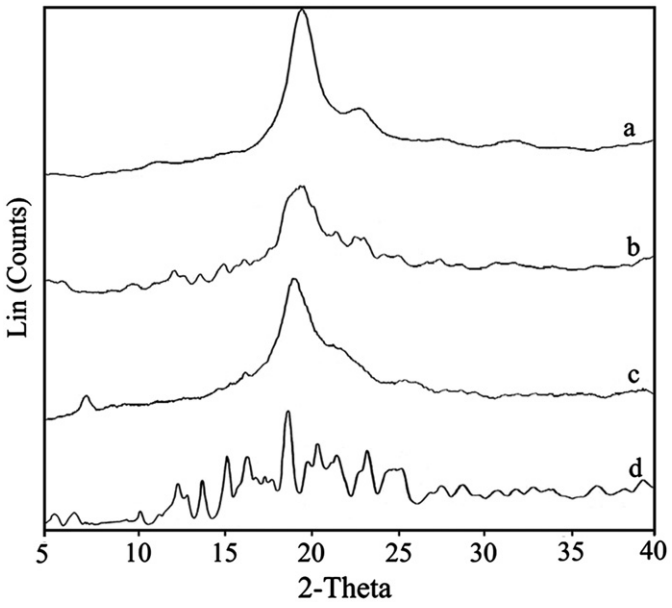

Fig. 6. X-ray diffraction patterns for (a) PVA, (b) PVA/γ-CD mixture, (c) CD-PPR and (d) pure γ-CD.

γ-CD at room temperature from $2\theta=5^\circ$ to 40°. The CD-PPR showed a diffraction pattern quite different from the diffractograms of PVA and γ-CD. Major peaks at approximately $2\theta=18.2$ were observed for pure γ-CD. The key feature was the peak at approximately $2\theta=7.1^\circ$ (curve *c*). As could be observed, this feature was not present in the pure γ-CD or in the physical mixture; it was only observed in the CD-PPR. This result strongly supports the inclusion of PVA chains within the cylindrical cavities of γ-CDs. Moreover, there was a strong diffraction peak at approximately $2\theta=19.2$ (curve *c*), which may be a possible indicator of γ-CD channels that include polymers inside [27].

3.2. Preparation of BSA imprinted polymer

Protein imprinted polymer nanowires and polymer nanofilaments have been prepared, and all of them have higher template binding capacities due to their binding sites on the surfaces of materials [28,29]. In this work, the configuration of the CD-PPRs, channels of shallow truncated cones traversed by ARPCs, was similar to that of polymer nanowires and was able to maintain its three-dimensional specific recognition cavities corresponding only to protein templates. Compared with the conventional supports used in protein molecular imprinting methods, CD-PPRs did not act as real supports. Actually, the conventional supports could offer sites for proteins recognition processes, such as the surfaces of microspheres or that of silica particles. So they were the real supports. But CD-PPRs only supplied relatively huge molecular combinations in the imprinted polymer matrix, which would benefit for template recognition. Therefore, we referred to the CD-PPRs as pseudo-supports.

To elucidate the function of CD-PPR in a polymer matrix, the amounts of CD-PPR used in the polymerisation reaction system were analysed first. The concentrations of CD-PPR tested varied from 30 to 120 mg mL^{-1}. The effect of the CD-PPR content on the adsorption of BSA is shown in Table 2. From Table 2, the amount of BSA adsorbed initially increased with the increase in the CD-PPR content and then decreased with the further increase in the CD-PPR content. Under the experimental conditions, the cp-MIP3 obtained showed maximal affinity toward the template when the CD-PPR content was 90 mg mL^{-1}.

Table 2
Results of BSA MIPs adsorption performed of varying CD-PPR content.

Samples[a]	CD-PPR (g)	Cu^{2+} (μL)	Q (mg g^{-1})
cp-MIP1	0.30	10.0	2.32
cp-MIP2	0.60	10.0	3.48
cp-MIP3	0.90	10.0	4.15
cp-MIP4	1.20	10.0	3.70
a-MIP	0	0	1.43
CD-MIP	1.00	0	1.89

[a] Sample quantity: 1.0 g; Concentration of BSA=0.500 mg mL^{-1}; Concentration of Cu^{2+}=0.500 mg mL^{-1}.

Table 3
Results of BSA MIPs adsorption performed of varying Cu ion content.

Samples[a]	CD-PPR (g)	Cu^{2+} (μL)	Q (mg g^{-1})
cp-MIP5	1.00	20.0	4.30
cp-MIP6	1.00	30.0	4.96
cp-MIP7	1.00	40.0	5.11

[a] Sample quantity: 1.0 g; Concentration of BSA=0.500 mg mL^{-1}; Concentration of Cu^{2+}=0.500 mg mL^{-1}.

Table 2 shows that the amount of BSA adsorbed increased initially and then decreased with the increase in the amount of CD-PPR. This result can be attributed to the CD-PPR configuration in the polymer matrix. As known, specific recognition sites are formed during the imprinting process, and previous studies have also demonstrated the importance of the spatial integrity of recognition cavities formed during the imprinting process [30]. In this case, when the CD-PPR complex was initially introduced during the polymerisation process, the spatial arrangement of the CD-PPR was beneficial in fixing the interactions among the protein template, monomer and cross-linkers. In other words, a large number of interactions benefited from protein recognition sites created within the protein template, monomer and the CD-PPR. Thus, many recognition sites and effective imprinted cavities could be fixed during the imprinting process. As a result, the specific adsorption to the template BSA was enhanced. A further increase in the amount of CD-PPR caused a decrease in the adsorbed amount because the higher CD-PPR content created the effect of space hampering. An excessive amount of cyclodextrins introduced would hamper the template approaching the monomers and cross-linkers; thus, the effective recognition network for the template was not liable to be created.

In addition to the CD-PPR mentioned above, metal ions were introduced and helped to form more stable complexes with the template molecules via multiple-site interactions. Metal ions and their role in coordinating specific binding in imprinted polymers have been reviewed elsewhere [30,31]. Among them, Cu ions utilized for the preparation of protein MIPs were relatively frequently and more successfully [32,33]. Interactions between biological molecules and metal ions can create three-dimensional specific recognition cavities corresponding to template proteins in polymer networks. Such interactions tend to be highly specific and usually reversible under mild reaction conditions [34,35]. In this study, Cu ions were employed to enhance recognition specificity during the protein imprinting process. Fortunately, when Cu ions were added to construct the MIPs network, the amount of BSA adsorbed increased (Table 3). Under the experimental conditions, the amount of BSA adsorbed increased with the increase in the Cu ion content.

3.3. Characterisation of MIPs

SEM was employed to capture the detailed morphology of the cp-MIP, *a*-MIP and NIP (Fig. 7). As shown in Fig. 7a and b, the NIP

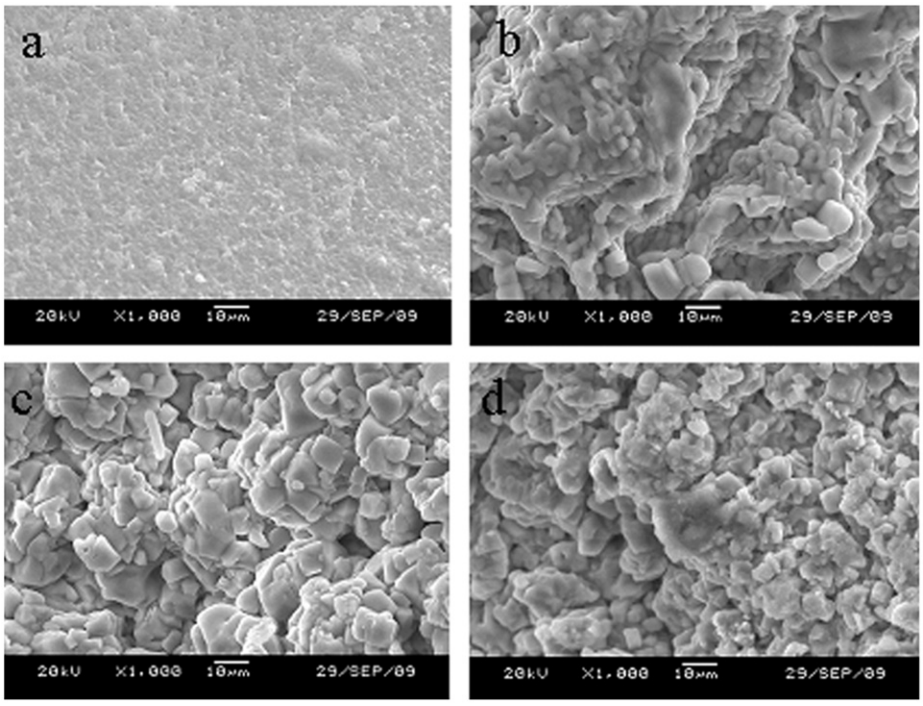

Fig. 7. SEM images of (a) NIP, (b) a-MIP, (c) CD-MIP and (d) cp-MIP.

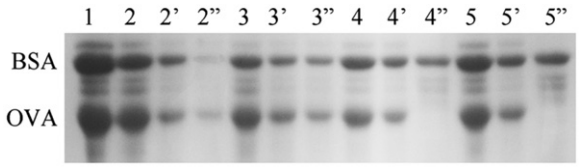

Fig. 8. SDS-PAGE analysis of proteins adsorbed onto NIP (2), a-MIP (3), CD-MIP (4) and cp-MIP3 (5): Lane 1, original mixture of BSA and OVA; Lanes 2, 3, 4, 5, proteins washed with 0.10 mol L^{-1} phosphate buffer; Lanes 2′, 3′, 4′, 5′, proteins washed with 0.15 mol L^{-1} KCl solution; Lanes 2″, 3″, 4″, 5″, proteins washed with 0.50 mol L^{-1} KCl solution. Ten microlitres of elute buffer was used in each Lane.

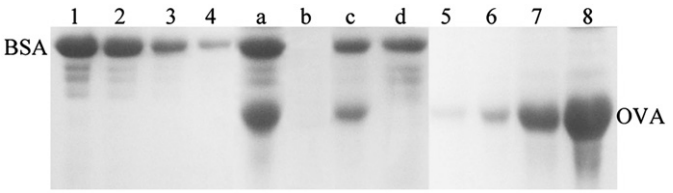

Fig. 9. SDS-PAGE analysis of the results for the isolation of BSA and OVA: Lanes 1–4, BSA standard, the concentration was 0.500, 0.250, 0.125, 0.0625 μg μL^{-1}, respectively; Lane a, 10 μL of protein mixture before adsorption (0.500 mg mL^{-1} each); Lane b, 10 μL of NIP eluent; Lane c, 10 μL of a-MIP eluent; Lane d, 10 μL of cp-MIP3 eluent; Lane 5-8, OVA standard, the concentration was 0.125, 0.250, 0.500, 1.00 μg μL^{-1}, respectively. Each of the standards used was 10 μL.

revealed smooth surface, while the a-MIP showed a grainy surface. After the CD-PPR complex was introduced into the polymer system, the cp-MIP also exhibited a rough and grainy surface, but the graininess fringe was relatively regular (Fig. 7c). The shape of the graininess fringe can be attributed to the truncated cones forming the γ-CD, which benefited the adsorption of the template protein. We inferred that the CD-PPR, with its relative rigidity may maintain a suitable configuration for protein imprinting.

3.4. Protein adsorption experiments

To obtain the specific adsorption protein, the MIPs and NIP were washed with different buffers (Fig. 8). In Fig. 8, proteins in Lane 2, 3, 4 and 5 were collected with 0.10 mol L^{-1} phosphate buffer, and proteins in Lane 2′, 3′, 4′ and 5′ were collected with 0.15 mol L^{-1} KCl solution. The protein content of each lane in each group (one group included lane 2, 3, 4 and 5; the other group included lane 2′, 3′, 4′ and 5′) showed no obvious differences. However, there were some distinctions among proteins eluted with 0.500 mol L^{-1} KCl solution in lane 2″, 3″, 4″ and 5″. Small amounts of protein were eluted from NIP (Lane 2″), while both BSA and OVA were eluted from a-MIP (Lane 3″). Only BSA was eluted from CD-MIP and cp-MIP3 (Lane 4″ and 5″). From these results, it was confirmed that the target BSA protein was eluted with 0.500 mol L^{-1} KCl solution. In particular, the amount of BSA imprinted increased when Cu ions were introduced into polymer matrix. The results can be attributed to the following: under the optimal binding conditions, the linear chelating assembly formed among CD-PPR skeletons, metal ions and the template proteins could best maintain the configuration matching the original imprinting state. Such a polymer matrix would be more suitable for the protein template on the molecular scale, and the recognition of the protein template would be highly specific. As a result, cp-MIP showed excellent specific adsorption, better than that exhibited by a-MIP without CD-PPR.

As stated above, in this work two methods were adopted to measure the amount of protein adsorbed by the polymers. One was UV/Vis spectrophotometer, the other was SDS-PAGE. The decreased protein content in the supernatant solutions measured with a UV/Vis spectrophotometer should include specific proteins and non-specific proteins adsorbed by the polymer.

It should be mentioned that it is very difficult to remove template proteins in current molecular imprinting methods because the highly cross-linked polymer matrix does not allow these molecules to move freely. Fortunately, due to CD-PPR, with its special configuration (channel of shallow truncated cones traversed by PVA chains), which was immobilised in this case, the BSA template was very easy to remove from the imprinted location in the polymer matrix.

For the BSA/OVA mixture, the amount of BSA adsorbed was determined by SDS-PAGE (Fig. 9). The protein competitor chosen

was OVA, which has a similar isoelectric point and similar molecular weight. Table 4 shows the selectivity factors (α) for BSA MIPs as OVA control protein. The maximum BSA adsorption capacity was about 600 μg g^{-1} polymers. The relative selectivity coefficient of cp-MIP for BSA/OVA was more than 6.6 times as that of *a*-MIP.

The analyses of the supernatants collected from the BSA adsorption experiments and from rebinding experiments were performed using a UV/Vis spectrophotometer. Table 5 shows the adsorbed amounts after several regeneration cycles. The results showed that the cp-MIP was very stable and maintained its adsorption ability at 96% of its capacity.

3.5. Selectivity experiments

To better demonstrate the specificity of the MIPs, BSA separation from the protein mixture was established by incubating the MIPs in buffer containing four proteins (BSA, OVA, SBTI and LYS). The MIPs were washed with 0.500 mol L^{-1} KCl solution to obtain the specific adsorption protein. The protein adsorbed and the residual solutions were analysed by SDS–PAGE (Fig. 10). The adsorption results shown in Fig. 10 clearly indicate that the cp-MIP exhibits much better purification performance than a-MIP (Lane 6, 7, 8).

By the preorganisation of the CD-PPR complex with BSA molecules in the presence of Cu ions, the functional groups can be ordered to a moderate degree in the polymer matrix, and the resultant cp-MIPs showed excellent specificity toward the templates in the original conformation. Consequently, this perhaps made these cavities the principal factor for protein recognition. Once the protein imprinted polymer formed, the specific recognition depended mainly on the shape memory effect. The skeleton formed by CD-PPR and metal ions, which is responsible for maintaining the cavity configuration, produced a rigid polymer matrix. A rigid polymer matrix should contain imprinting cavities with a better defined shape and result in MIPs with higher specificity [36]. In contrast to that of traditional MIPs on supports, the relative position of the functional groups corresponding to template protein should be controlled easily via the CD-PPR-Cu^{2+} complex. The recognition of the template would be specific when the MIPs maintain a 3D structure, as in the imprinting process [37]; thus, nonspecific interactions with proteins were expected to be minimised in this matrix.

Table 4
Selectivity factors for BSA MIPs using OVA as control protein.

	Adsorption materials[a]			
	a-MIP		cp-MIPs	
	BSA	OVA	BSA	OVA
Binding amounts, μg	1.41	> 3.13	1.88	< 0.625
Selectivity factor, α[b]	< 0.450		> 3.00	
Relative selectivity coefficient[c]		> 6.6		

[a] 10 μL of eluent is calculated in this table.
[b] The selectivity factor is calculated using the following formula: α = value of BSA/value of OVA.
[c] Relative selectivity coefficient is calculated with $\alpha_{cp\text{-}MIP3}/\alpha_{cp\text{-}MIP3}$.

Table 5
Adsorption results of BSA rebinding experiments with different polymer types.

Samples[a]	Adsorption capacity (mg g^{-1})			
	Cycle 1	Cycle 2	Cycle 3	Cycle 4
cp-MIP3	4.15	4.11	4.05	3.98
CD-MIP	1.89	1.82	1.77	1.68
a-MIP	1.43	1.29	1.16	1.07

[a] Sample quantity: 1.0 g; Concentration of BSA = 0.500 mg mL^{-1}; Volume of BSA solution = 10.0 mL.

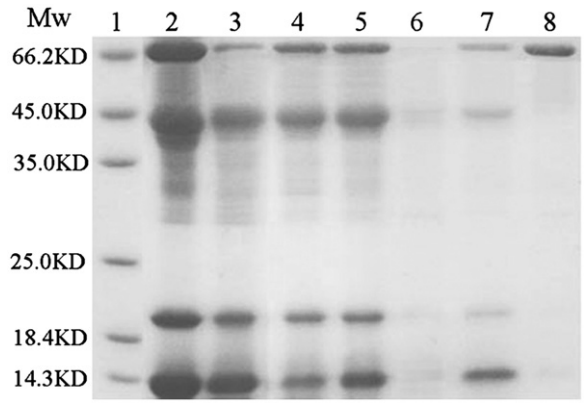

Fig. 10. SDS-PAGE analysis of the results for the isolation of BSA from a mixture of four proteins using the protein-imprinted polymer: Lane 1, protein molecular weight marker; Lane 2, 10 μL of protein mixture containing BSA (target protein), OVA, SBTI and LYS (0.500 mg mL^{-1} each) before adsorption. Lanes 3–5, 10 μL of residual solution after adsorption by cp-MIP, a-MIP and NIP, respectively. Lanes 6–8, 10 μL of elute buffer by NIP, a-MIP and cp-MIP, respectively.

4. Conclusion

In conclusion, we have developed a novel approach to prepare protein MIPs with CD-PPRs as pseudo-supports and thereby a highly effective recognition system. The configuration exhibited by this framework combined with multi-chemical interactions facilitates the linear chelation among ARPCs, metal ions, and cyclodextrins. Unlike the other approaches employed for protein molecular imprinting, this approach focuses on enhancing the force of recognition sites and on the three-dimensional structure of the support. It utilises a diversity of CD-PPRs based on the molecular weight of ARPCs and/or the number of CDs assembling with ARPCs. We intended to discuss the imprinting effect with respect to the space configuration of MIPs and the three-dimensional scale of the support in the MIPs matrix. The results support our theory that the recognition specificity to the template protein relies mainly on the spatial configuration created by CD-PPR and metal ions. Using this approach, not only can we solve the problem of the template being difficult to eliminate in the conventional embedding method but the imprinting amount is also increased using this surface imprinting method. This approach would also provide valuable information on the design and construction of desired supramolecular structures and functions for the separation and purification of proteins. Future studies should focus on the effect of the length of CD-PPR on recognition specificity and on the confirmation of the exact recognition sites within the polymer matrix.

Acknowledgements

This work was supported by the National Natural Science Foundation of China (No. 20704031, No. 20974053 and No. 21004034) and Tianjin Municipal Natural Science Foundation of China (No. 11JCYBJC03900).

References

[1] H. Nishino, C.-S. Huang, K.J. Shea, Angew. Chem. Int. Ed. 45 (2006) 2392–2396.
[2] D.E. Hansen, Biomaterials 28 (2007) 4178–4191.
[3] Y. Zheng, X. Wang, Y.B. Ji, Talanta 91 (2012) 7–17.
[4] D.S. Janiak, O.B. Ayyub, P. Kofinas, Macromolecules 42 (2009) 1703–1709.
[5] E. Verheyen, J.P. Schillemans, M.V. Wijk, M.-A. Demeniex, W.E. Hennink, C.F.V. Nostrum, Biomaterials 32 (2011) 3008–3020.
[6] D.R. Kryscio, N.A. Peppas, Acta Biomater. 8 (2012) 461–473.
[7] E. Yilmaz, O. Ramstrom, P. Moller, D. Sanchez, K. Mosbach, J. Mater. Chem. 12 (2002) 1577–1581.
[8] T. Shiomi, M. Matsui, F. Mizukami, K. Sakaguchi, Biomaterials 26 (2005) 5564–5571.
[9] W.J. Xu, S.F. Su, P. Jiang, H.S. Wang, X.C. Dong, M. Zhang, J. Chromatogr. A 1217 (2010) 7198–7207.
[10] A. Bossi, S.A. Piletsky, E.V. Piletska, P.G. Righetti, A.P.F Turner, Anal. Chem. 73 (2001) 5281–5286.
[11] T.Y. Guo, Y.Q. Xia, J. Wang, M.D. Song, B.H. Zhang, Biomaterials 26 (2005) 5737–5745.
[12] S.A. Mourouzidis-Mourouzis, A.J. Karabelas, J. Membr., Sci 282 (2006) 124–132.
[13] A. Bossi, F. Bonini, A.P. Turner, S.A. Piletsky, Biosens. Bioelectron. 22 (2007) 1131–1137.
[14] K.E. Kirat, M. Bartkowski, K. Haupt, Biosens. Bioelectron. 24 (2009) 2618–2624.
[15] B.J. Gao, H.Y. Fu, Y.B. Li, R.K. Du, J Chromatogr, B Analyt Technol, Biomed. Life Sci. 878 (2010) 1731–1738.
[16] W. Zhang, X.W. He, Y. Chen, W.Y. Li, Y.K. Zhang, Biosens. Bioelectron. 26 (2011) 2553–2558.
[17] A. Harada, Y. Takashima, H. Yamaguchi, Chem. Soc. Rev. 38 (2009) 875–882.
[18] I.N. Topchieva, I.G. Panova, V.V. Spiridonov, E.V. Matukhina, B.I. Kurganov, Colloid J 71 (2009) 550–558.
[19] D. Thompson, J.A. Larsson, J. Phys. Chem. B 110 (2006) 16640–16645.
[20] T. Osawa, K. Shirasaka, T. Matsui, S. Yoshihara, T. Akiyama, T. Hishiya, Macromolecules 39 (2006) 2460–2466.
[21] W. Zhang, L. Qin, X.W. He, W.Y. Li, Y.K. Zhang, J. Chromatogr. A 1216 (2009) 4560–4567.
[22] R. Hernandez, M. Rusa, C.C. Rusa, D. Lopez, C. Mijangos, A.E. Tonelli, Macromolecules 37 (2004) 9620–9625.
[23] G. Andrade, E.F. Barbosa-Stancioli, A.A. Piscitelli Mansur, W.L. Vasconcelos, H.S. Mansur, Biomed. Mater. 4 (2006) 221–234.
[24] M.J. Guo, Z. Zhao, Y.G. Fan, C.H. Wang, L.Q. Shi, J.J. Xia, H.F. Mi, Biomaterials 27 (2006) 4381–4387.
[25] J.J. Xia, Y. Long, M.J. Guo, Y. Wang, H.F. Mi, Sci. Chin. Ser. B 52 (2009) 1388–1393.
[26] M.J. Guo, T. Gao, Z. Fan, J.X. Yao, J.J. Xia, H.F. Mi, Sci. Chin. Ser. B 53 (2010) 905–911.
[27] A. Harada, J. Li, M. Kamachi, Polym. Adv., Technology 8 (1997) 241–249.
[28] Y. Li, H.H Yang, Q.H You, Z.X. Zhuang, X.R Wang, Anal. Chem. 78 (2006) 317–320.
[29] A.V. Linares, F. Vandevelde, J. Pantigny, A. Falcimaigne-Cordin, K. Haupt, Adv. Funct. Mater. 19 (2009) 1299–1303.
[30] N.W. Turner, C.W. Jeans, K.R. Brain, C.J. Allender, V. Hlady, D.W. Britt, Biotechnol. Progr. 22 (2006) 1474–1489.
[31] II.P.G. Conrad, K.J. Shea, Molecularly Imprinted Materials: Science and Technology, Marcel Dekker, Inc., New York, 2005, pp.123-180.
[32] A.A. Ozcan, R Say, A. Denizli, A. Erso1z, Anal. Chem. 78 (2006) 7253–7258.
[33] L. Qin, X.W. He, W. Zhang, W.Y. Li, Y.K. Zhang, Anal. Chem. 81 (2009) 7206–7216.
[34] N. Bereli, M. Andac, G. Baydemir, R. Say, I.Y. Galaev, A. Denizli, J. Chromatogr. A 1190 (2008) 18–26.
[35] J.Q. Liu, G. Wulff, J. Am. Chem. Soc. 126 (2004) 7452–7453.
[36] E.V. Piletska, A.R. Guerreiro, M.J. Whitcombe, S.A. Piletsky, Macromolecules 42 (2009) 4921–4928.
[37] C.J. Tan, Y.W. Tong, Langmuir 23 (2007) 2722–2730.